

# Recent applications of sliding block theory to geotechnical design

Hoe I. Ling

*Department of Civil Engineering and Engineering Mechanics, Columbia University, 500 West 120th Street, New York, NY 10027, USA*

Accepted 17 January 2001

## Abstract

The sliding block theory was proposed by Newmark for determining the permanent displacement of embankments and dams under earthquake loading. This paper highlights recent applications of sliding block theory to different geotechnical structures. The equations to determine seismic factor of safety, yield acceleration and permanent displacement are given for rock block, soil slope, landfill cover, geosynthetic-reinforced soil retaining wall, and composite breakwater. The presented equations for seismic stability degenerate to that of static stability in the absence of earthquake. The permanent displacement for various structures can be obtained from that of a horizontal sliding block through a correction factor. A simplified procedure is included for the permanent displacement under vertical acceleration. The sliding block approach is rational for design under high seismic load. © 2001 Elsevier Science Ltd. All rights reserved.

*Keywords:* Sliding block; Permanent displacement; Seismic stability; Slope; Reinforced soil; Landfill; Breakwater

## 1. Sliding block theory

Newmark [25] proposed the sliding block theory and illustrated its application to embankments and dams under seismic loading. The same theory was proposed by Whitman as included in a letter submitted by Taylor to the US Army Corps of Engineers [24]. In the sliding block theory, soil is assumed to be rigid-plastic and slides along a prescribed planar failure surface. The earthquake inertia force is assumed pseudo-static as expressed by a seismic coefficient, which is a fraction of the weight of potential sliding soil mass. The yield or critical acceleration is defined for the soil mass at the limit state where the factor of safety against sliding equal to unity. During seismic excitation, sliding accumulates whenever this yield value is exceeded. Newmark suggested that displacement may be neglected for the reverse acceleration since the yield value in the reversed direction is typically very large. Thus, a permanent displacement is evaluated for the soil mass subject to earthquake acceleration. The momentary failure may or may not jeopardize the performance of the structure depending on the acceptable displacement limit.

Newmark theory has been verified to a certain extent in the mid 1960s. The theory was found valid for the slopes having a thin layer of sand and subject to seismic shaking [5,28]. The theory has been proposed for practical design of earth dam [2,6,23]. The idea of permanent displacement limit has also been used to design seismically other types of geotechnical structures, such as retaining walls [26,29].

Despite continued efforts made in improving seismic

design, mainly through pseudo-static analysis with a factor of safety, deformations ranging from slight displacement to catastrophic failure have been observed in many earth structures during major earthquakes. The Northridge and Kobe earthquakes left over many controversial issues, such as the seismic coefficient used in design and the effect of vertical acceleration. Following Kobe earthquake, a seismic coefficient as large as 0.8 has been proposed in Japan for structures designed to resist a Level 2 earthquake [9]. For earth structures, the large seismic coefficient implies that conventional pseudo-static design is infeasible if Level 2 design will be implemented. Therefore, alternate design methodologies are sought. Koseki et al. [11] proposed a modified procedure to Mononobe-Okabe analysis for retaining wall design where the failure plane is determined by the peak frictional angle but the strength is based on the residual value. On the contrary, performance-based design, using permanent displacement, has been examined by Ling and Leshchinsky [20], among other researchers, for different earth structures to counter for high seismic load. The author does notice that several Japanese authorities, such as those dealing with railway embankment, retaining walls, and earth dams, are recently pursuing research in the area of implementing permanent displacement to design [8].

In this paper, the sliding block theory is examined further from two perspectives: recent applications to geotechnical structures and inclusion of vertical acceleration. The application of sliding block theory to new emerging geotechnical structures, including geosynthetic-reinforced soil retaining

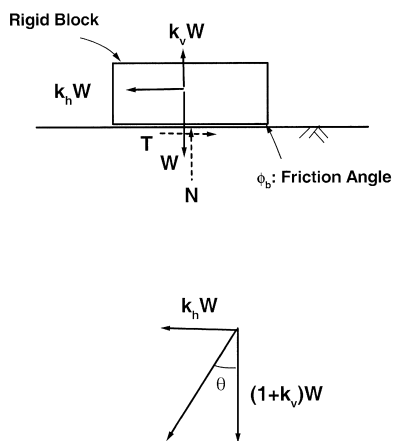


Fig. 1. Rigid block sliding along a horizontal plane.

walls and landfill cover liners, as well as traditional structures, such as earth and rock slopes, is described.

## 2. Yield acceleration and permanent displacement

The yield acceleration can best be illustrated by a rigid block resting on a horizontal plane (Fig. 1). Let  $W$ ,  $k_h$ ,  $k_v$  and  $\phi$  be the weight of the block, horizontal and vertical coefficients of acceleration, and angle of friction between the block and the plane, respectively. The force equilibrium equations are assembled to give the traction and normal force  $T = k_h W$  and  $N = (1 - k_v)W$ , respectively. The interface surface friction is governed by Coulomb's law:  $T = \tan\phi N$ . At limit state, coefficient of yield horizontal acceleration is obtained as

$$k_{hy} = (1 - k_v)\tan\phi \quad (1)$$

Thus, the yield acceleration depends on the friction angle and the magnitude and direction of vertical acceleration, which varies with time. In this simple case, the vertical acceleration that acts upward reduces the yield acceleration. If  $k_v$  acts downward, the coefficient of yield acceleration is

$$k_{hy} = (1 + k_v)\tan\phi \quad (1')$$

If the earthquake acceleration exceeds the yield acceleration of the block, sliding occurs. The equation of motion is established to give the acceleration of the block. The displacement is obtained by double integrating the acceleration:

$$x = \iint (k_h - k_{hy})g \cdot dt \quad (2)$$

Fig. 2(a) shows typical vertical and horizontal accelerations obtained from Kobe earthquake. The peak horizontal and vertical accelerations are  $k_{ho} = 0.63$  g and  $k_{vo} = 0.34$  g, respectively. An example is illustrated with  $\phi = 20^\circ$ , where  $\phi$  is the angle of friction along the direction of motion. A large frictional resistance in the reverse direction is assumed. If the vertical acceleration is neglected,

$k_{hy} = 0.364$ , else  $k_{hy}$  varies with time, as indicated in the Fig. 2(a). Fig. 2(b) shows the relationships between velocity and displacement for the rigid block. There are a few occasions where earthquake acceleration exceeds the yield acceleration, thus induces motion. The permanent displacement is calculated as 8.1 cm. By scaling the earthquake record with different values of peak accelerations, the relationships between displacement  $x$  and  $k_{ho} - k_{hy}$ , were determined numerically and presented in Fig. 3. Consequently, by estimating the peak acceleration of the earthquake and knowing the yield acceleration of the block, the permanent displacement can be determined graphically from Fig. 3 for given earthquakes.

The sliding block theory may be applied to different failure mechanisms. In this paper, the applications involve extending the static analysis to seismic analysis via pseudo-static approach. The failure of slopes is considered through two different mechanisms: planar and non-planar mechanisms. In the planar mechanism, the slidings of rock block and soil slope are considered. The planar mechanism involving a two-part wedge is applied to the cover liner of the landfill and geosynthetic-reinforced soil retaining wall. The application of log-spiral mechanism is illustrated through soil slope. Finally, pseudo-static analysis and sliding block theory are applied to breakwater caisson. In all cases of application, the yield acceleration and permanent displacement are discussed.

Two functions,  $k$  and  $\theta$ , that are related to seismic coefficients (Fig. 1), will be used in this papers.

$$k = \sqrt{k_h^2 + (1 \pm k_v)^2} \quad (3a)$$

$$\tan\theta = \frac{k_h}{1 \pm k_v} \quad (3b)$$

where vertical acceleration may act upward or downward depending on the formulation. The selection of the direction of  $k_v$  is based on the most critical conditions, and will be discussed for each case of application.

## 3. Rock wedge stability

The sliding of rock block normally occurs along a well defined plane of weakness, such as joint. The joint plane may intercept a tension crack with the pore water pressure in the plane and in the crack (Fig. 4). A factor of safety against sliding is typically determined for the block [7]. Ling and Cheng [17] extended Hoek–Bray procedure to seismic conditions. The notations used by Hoek and Bray are adopted herewith.

The slope is homogeneous, of height  $H$  and with a unit weight  $\gamma$ . The slope face and joint plane are inclined at an angle (dip)  $\psi_f$  and  $\psi_p$ , respectively. The cohesion and angle of friction of the joint plane are  $c$  and  $\phi$ , respectively. The depth of the tension crack and depth of water in it are  $z$ , and  $z_w$ , respectively. In Fig. 5,  $W$ ,  $C$ ,  $T$ ,  $U$  and  $V$  are the weight of

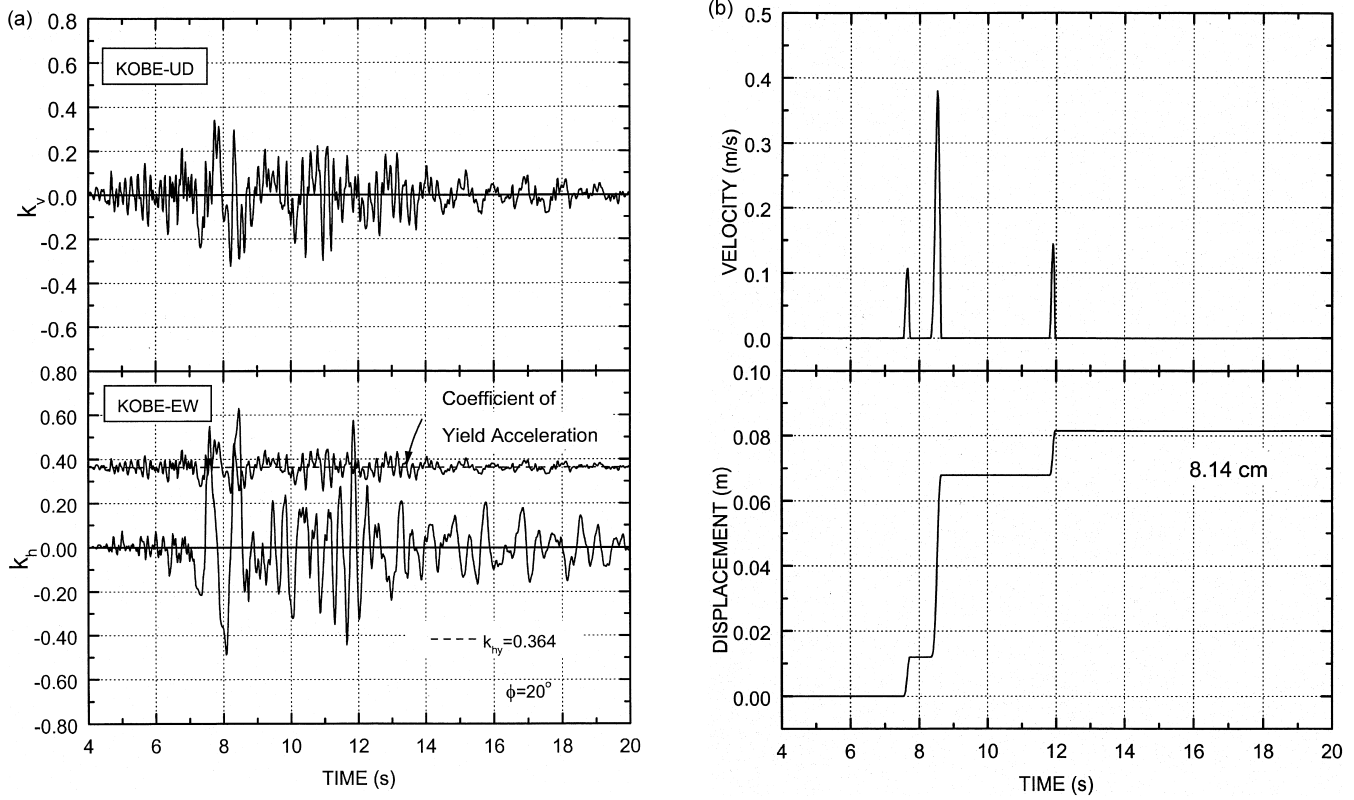


Fig. 2. (a) Kobe earthquake accelerations, (b) velocity and displacement.

the block, total cohesion and frictional resistance along the joint plane, pore water resultant force along the plane and in the tension crack, respectively. The factor of safety under seismic conditions is obtained in Eq. (4) through four dimensionless parameters,  $P'$ ,  $Q'$ ,  $R'$  and  $S'$ .

$$F_{sd} = \frac{\{Q' \cot(\Psi_p + \theta) - R'(P' + S')\} \tan \phi + \frac{2c}{\gamma H} P'}{Q' + R' S' \cot \Psi_p} \quad (4)$$

where

$$P' = \frac{1 - z/H}{\sin \Psi_p} \quad (5a)$$

$$Q' = \left\{ \frac{1 - (z/H)^2}{\tan \Psi_p} - \frac{1}{\tan \Psi_r} \right\} \sin(\Psi_p + \theta) \quad (5b)$$

$$R' = \frac{\gamma_w z_w}{\gamma H} \quad (5c)$$

$$S' = \frac{z_w \sin \Psi_p}{H} \quad (5d)$$

Note that the expression  $Q'$  above is for the tension crack located behind the slope face. A list of figures were presented by Ling and Cheng [17] on the dimensionless

parameters for different slope geometries and properties. In the absence of seismic force,  $P'$ ,  $Q'$ ,  $R'$  and  $S'$  degenerate to  $P$ ,  $Q$ ,  $R$ , and  $S$  of Hoek–Bray’s equation. Also, for a dry slope ( $z_w = 0$ ,  $R' = S' = 0$ ), the seismic factor of safety is obtained as

$$F_{sd} = \frac{\tan \phi}{\tan(\Psi_p + \theta)} + \frac{2c}{\gamma H} \frac{P'}{Q'} \quad (6)$$

For  $c = 0$ , the seismic factor of safety (Eq. (6)) may be viewed as an increase of the inclination of joint plane by an angle  $\theta$ , i.e. from  $\psi_p$  to  $\psi_p + \theta$  such that the stability is reduced compared to the static case. The logic could be the basis for tilting table test although it is not discussed in the literature.

The yield seismic coefficient for the block, without considering pore water pressure is

$$k_{ny} = (1 + k_v) \tan(\phi - \Psi_p) + \frac{C}{\eta W} \quad (7)$$

where

$$C = cH \left\{ \frac{1 - z/H}{\sin \Psi_p} \right\} \quad (8)$$

$$\eta = \frac{\cos(\phi - \Psi_p)}{\cos \phi} \quad (9)$$

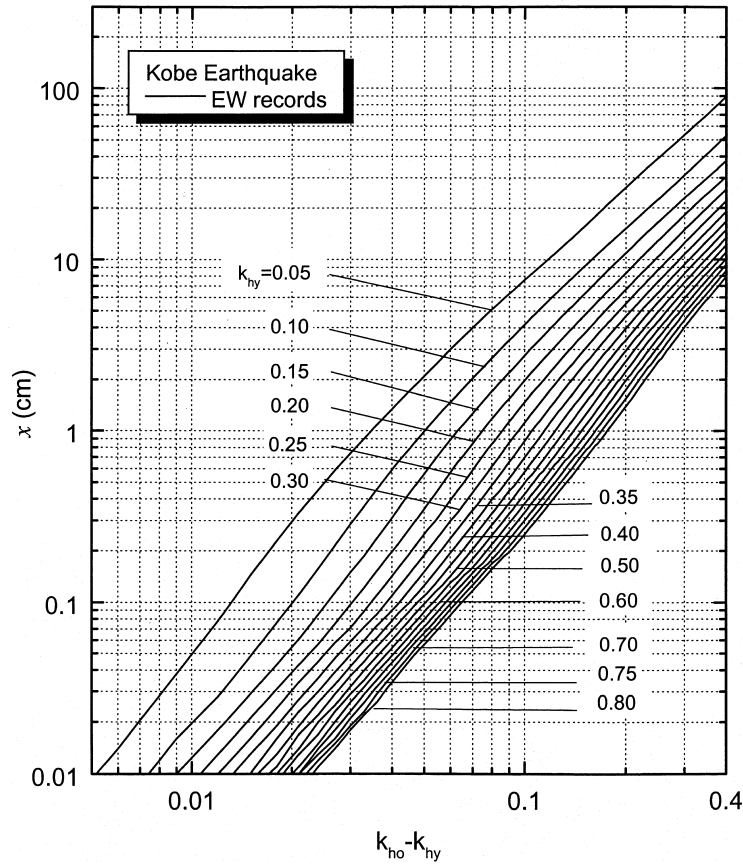


Fig. 3. Rigid block sliding along horizontal plane.

In the absence of cohesion,  $k_{hy}$  degenerates to

$$k_{hy} = (1 + k_v)\tan(\phi - \Psi_p) \tag{10}$$

The equation shows that for an inclined failure plane, the decrease in yield acceleration may be viewed as an equivalent decrease in the angle of friction from  $\phi$  to  $\phi - \psi_p$ .

The permanent sliding of the block along the plane is determined by double integrating the equation of

motion:

$$l = \eta \int \int (k_h - k_{hy})g \cdot dt \tag{11a}$$

$$\eta = \frac{\cos(d - \psi_p)}{\cos \phi} \tag{11b}$$

Eq. (11) may be obtained graphically from Fig. 3, or for

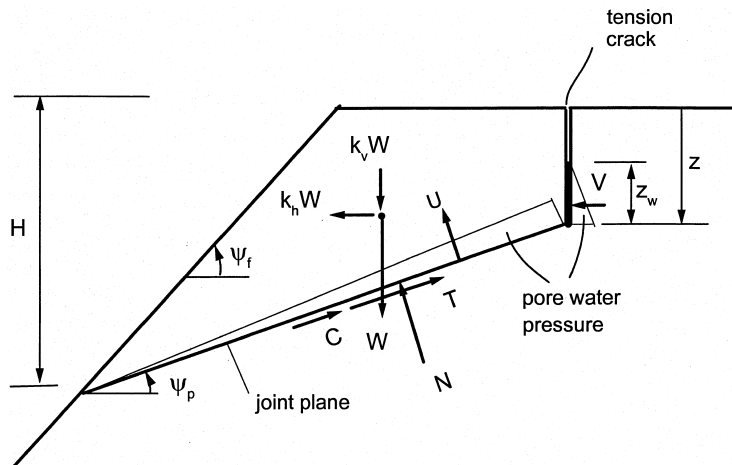


Fig. 4. Sliding of rock block along joint plane.

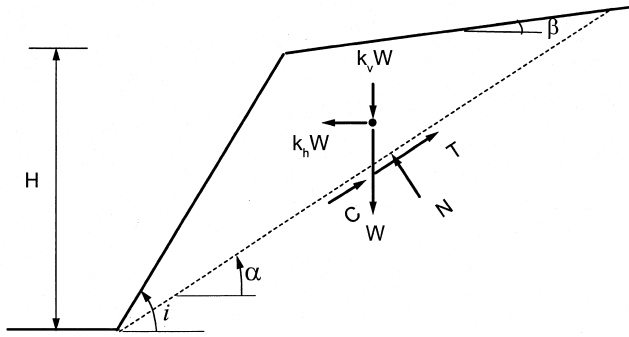


Fig. 5. Sliding of soil wedge along most critical plane.

any earthquake records, by applying a correction factor  $\eta$  to the displacement obtained in a horizontal sliding block (see Eq. (2)).

#### 4. Slope stability

##### 4.1. Planar mechanism

The equations obtained for rock block stability may be used for soil slopes if the failure plane is well defined. However, it is a common practice in slope stability analysis to seek for the factor of safety along the most critical failure plane. Ling et al. [22] extended Francais–Culmann analysis to seismic conditions for a slope inclined at an angle  $i$  (Fig. 5). The crest is inclined at an angle  $\beta$ . The most critical failure plane is determined at an inclination

$$\alpha = \frac{i + \phi - \theta}{2} \quad (12)$$

The dimensionless stability number is obtained as

$$N = \frac{c}{\gamma H} = \frac{1 + k_v}{4} \frac{\{1 - \cos(\phi - i - \theta)\} \cos \beta}{\cos \theta \cos \phi \sin(i - \beta)} \quad (13)$$

The yield seismic coefficient along the failure plane is obtained as

$$k_{hy} = (1 + k_v) \tan(\phi - \alpha) + \frac{\sin i \cos \phi}{\sin(i - \alpha) \cos(\phi - \alpha)} \frac{2c}{\gamma H} \quad (14)$$

The permanent displacement is obtained from Eq. (11), but with  $\psi_p$  replaced by  $\alpha$ . Note that the stability number obtained from Eq. (13) is very close to log-spiral mechanism for steep slopes [18].

##### 4.2. Log-spiral mechanism

The non-planar mechanism is more representative of the real slope failure. Sarma [27] used a circular failure surface whereas log-spiral has been used by Chang et al. [1]. A log-spiral mechanism with variational approach has been used by Leshchinsky and San [13]. The procedure has been extended to consider seismic displacement [15] and with the inclusion

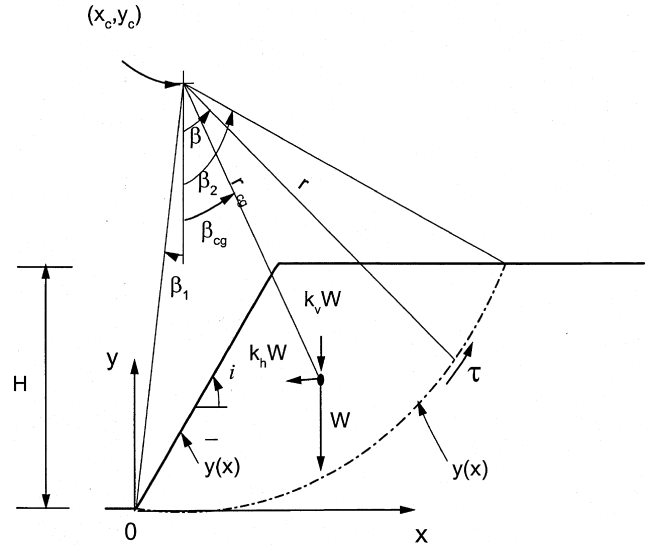


Fig. 6. Rotational sliding of soil slope.

of vertical acceleration [18]. The formulation uses dimensionless coordinates ( $X = x/H$ ,  $Y = y/H$ ) and strength ( $N_m = c/\gamma H F_s$ ,  $\phi_m = \tan \phi/F_s$ ), with the soil mass bounded between angles  $\beta_1$  and  $\beta_2$  for the slope surface  $\bar{Y}(X)$  and failure surface  $Y(X)$  (Fig. 6). The moment equilibrium equation is written at the pole of log-spiral  $(X_c, Y_c)$  as

$$\begin{aligned} N_m \int_{\beta_1}^{\beta_2} [(Y - Y_c) - (X - X_c) dY/dX] (\cos \beta \\ - \Psi_m \sin \beta) \exp(-\beta \Psi_m) d\beta + (1 + k_v) \int_{\beta_1}^{\beta_2} (\bar{Y} - Y)(X - X_c) \\ \times (\cos \beta - \Psi_m \sin \beta) \exp(-\beta \Psi_m) d\beta + \frac{k_h}{2} \int_{\beta_1}^{\beta_2} (\bar{Y} - Y) \\ \times (Y + \bar{Y} - 2Y_c) (\cos \beta - \Psi_m \sin \beta) \exp(-\beta \Psi_m) d\beta = 0 \end{aligned} \quad (15)$$

where the first, second and third terms represent contributions of the soil shear strength, weight of soil with vertical seismic force and horizontal seismic force, respectively.

Because of complexity of Eq. (15), a computer program is more relevant to solve for  $N_m$  with the slopes of different geometry and properties. Likewise, the yield acceleration may also be determined numerically from Eq. (15), with  $F_s$  equal to unity.

By assuming small rotation and neglect the change of yield acceleration with the change in geometry, the angular acceleration of the failure soil mass is obtained as:

$$\ddot{\theta} = \eta_\theta (k_h - k_{hy}) g \quad (16)$$

where

$$\eta_\theta = \frac{\cos \beta_{cg}}{r_{cg}} \quad (17)$$

where  $r_{cg}$  is the distance from the center of gyration to the

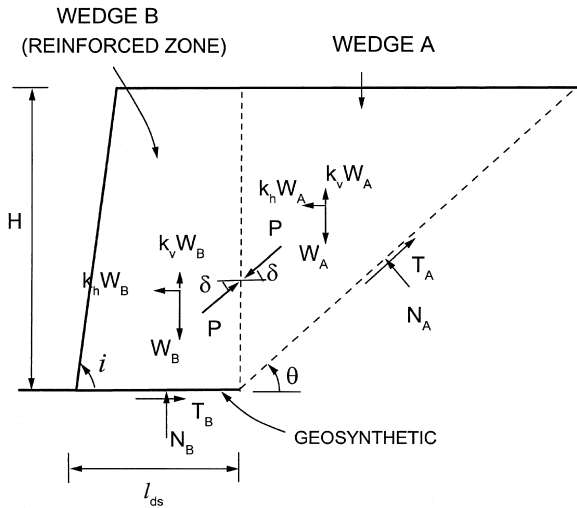


Fig. 7. Direct sliding of reinforced soil retaining wall.

pole of log-spiral, and  $\beta_{cg}$  is the inclination of the center of gyration measured from the vertical (Fig. 5).

The rotation of the soil mass is obtained by double integrating Eq. (16), from which the horizontal and vertical permanent displacements may be calculated at any point along the log-spiral. Again, the procedure is equivalent to applying a correction factor  $\eta_\theta$  to Eq. (2).

### 5. Geosynthetic-reinforced soil retaining wall

The design of reinforced soil retaining walls encompasses several different components, such as the internal stability that gives the length and strength of geosynthetic layers against rupture and pullout, and the external stability against direct sliding and over-turning [12,14]. The procedure of internal stability analysis can be conducted with Rankine/Coulomb analysis or using a rigorous log-spiral analysis. For direct sliding, a two-part wedge mechanism is commonly used.

Ling et al. [19] and Ling and Leshchinsky [20] extended the original procedure of Leshchinsky for a seismic design of geosynthetic-reinforced soil retaining walls. The two-part wedge direct sliding mechanism is shown in Fig. 7. Note that the most critical acceleration against direct sliding acts in the upward direction. In a series of parametric studies, it was found that direct sliding along the base of retaining wall could be the most critical considering large acceleration, especially if the vertical acceleration is included. The large acceleration may render design impossible due to lack of stability. Consequently, a performance-based design should be employed to avoid excessive length of geosynthetic layer needed to resist direct sliding.

The coefficient of yield acceleration of reinforced soil block is determined as

$$k_{hy} = (1 - k_v) \frac{W_B C_{ds} \tan \phi + W_A \tan(\phi - \alpha) \Lambda}{W_B + W_A \Lambda} \quad (18)$$

where

$$\Lambda = \frac{1 - C_{ds} \tan \delta \tan \phi}{1 - \tan \delta \tan(\phi - \alpha)} \quad (19)$$

$C_{ds} = \tan \phi_g / \tan \phi$  is the interaction coefficient, which expresses the ratio of frictional strength between soil-geosynthetic to that of soil.  $W_A$  and  $W_B$  are the weights of reinforced soil and potential sliding backfill soil,  $\delta$  is the interwedge friction angle (equal to  $\phi$  or  $\phi/2$ , or any other value).  $\alpha$  is the angle of inclination of the most critical failure plane, which may be determined numerically or using the expression of Richards and Elms [26].

The horizontal displacement for any given earthquake records may be obtained from Eq. (2). Ling et al. [19] and Ling and Leshchinsky [20] compared the approach with the performance of several geosynthetic-reinforced soil retaining walls. The comparison illustrated that the use of a tolerable displacement limit improves the design of geosynthetic-reinforced soil retaining wall.

### 6. Landfill cover liner

Geomembrane is used as liquid barrier in the waste containment. It is covered by a layer of cohesive soil that as protection medium. Because of the low frictional resistance between soil and geomembrane, the failure of cover soil typically occurs along the soil-geomembrane interface. It may also occur along the interface of geosynthetics depending on the interface strength. The static stability analysis of landfill cover soil, considering end effect (finite slope), has been presented by Giroud and Beech [3] and Koerner and Hwu [10]. The Koerner-Hwu approach is extended to include seismic loading. These formulations are based on a two-part wedge mechanism with the interwedge force acting parallel to the slope angle (Fig. 8). Note that the positive vertical acceleration is assumed to act upward.

The factor of safety of the cover soil to resist direct sliding is determined as

$$F_{ds} = \frac{T_A + P + k_v W_A \sin \beta + C_a}{W_A (k_h \cos \beta + \sin \beta)} \quad (20)$$

where

$$T_A = C_{ds} \tan \phi \{ (1 - k_v) \cos \beta - k_h \sin \beta \} W_A \quad (21)$$

$$P = \frac{W_B \{ (1 - k_v) \tan \phi - k_h \} + C}{\eta} \quad (22)$$

$$\eta = \frac{\cos(\phi + \beta)}{\cos \phi} \quad (23)$$

$$W_A = \gamma H L; \quad W_B = \frac{\gamma H^2}{\sin 2\beta}; \quad C = c \frac{H}{\sin \beta}; \quad C_a = c_a L \quad (24)$$

$W_A$  and  $W_B$  are the weight of the soil wedges,  $c_a$  is the

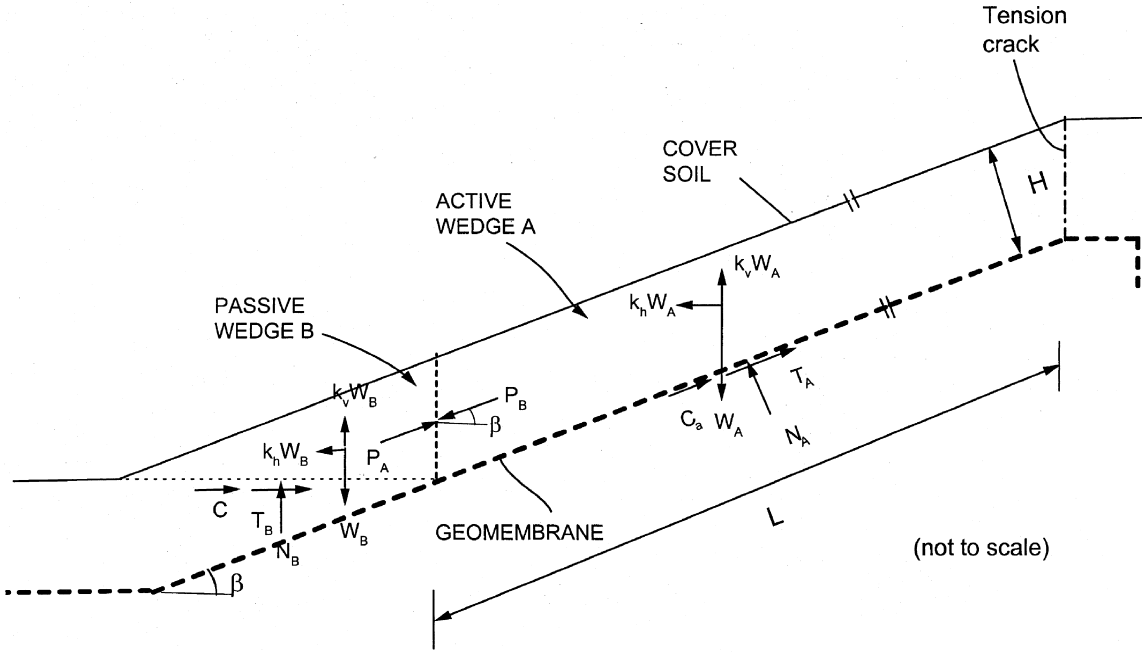


Fig. 8. Sliding of landfill cover liner.

adhesion between soil and geomembrane. The other notations are common to those presented in earlier sections.

From Eq. (20), the coefficient of yield acceleration is determined as

$$k_{hy} = \frac{(1 - k_v)\{W_A \eta(C_{ds} \tan \phi \cos \beta - \sin \beta) + W_B \tan \phi\} + C_a \eta + C}{W_A \eta (\cos \beta + C_{ds} \tan \phi \sin \beta) + W_B} \quad (25)$$

The displacement along the soil-geomembrane interface is obtained as

$$l = \eta' \int \int (k_h - k_{hy}) g \cdot dt \quad (26)$$

where

$$\eta' = \cos \beta + C_{ds} \tan \phi \sin \beta + \frac{H}{L \eta \sin 2\beta} \quad (27)$$

When the end effect is neglected (infinite slope), Eqs. (20), (25) and (27) degenerate to the following expressions:

$$F_{ds} = \frac{C_{ds} \tan \phi (1 - k_v - k_h \sin \beta) + k_v \tan \beta + c_a / \gamma H \cos \beta}{k_h + \tan \beta} \quad (28)$$

$$k_{hy} = \frac{(1 - k_v)(C_{ds} \tan \phi - \tan \beta) + c_a / \gamma H \cos \beta}{1 + C_{ds} \tan \phi \tan \beta} \quad (29)$$

$$\eta' = \cos \beta + C_{ds} \tan \phi \sin \beta \quad (30)$$

A series of parametric studies relating permanent displacement to the configuration and properties of cover system, for different earthquake records, are presented in Ling and Leshchinsky [16].

## 7. Composite breakwater

The stability of composite breakwater is determined based on a factor of safety against direct sliding. The major external forces acting on it are the lateral and uplift forces generated by the wave. Goda [4] proposed that  $P$  and  $U$  follow a trapezoidal and triangular pressure distribution (Fig. 9). The equations to determine  $P$ ,  $U$  and related coefficients are summarized in Ling et al. [21].

The factor of safety against direct sliding is obtained from the following equation:

$$F_s = \mu \frac{W' - U}{P} \quad (31)$$

$W'$  is the effective weight of the caisson,  $\mu$  is the coefficient of friction between the caisson and rubble mound (typically taken as 0.6).

Ling et al. [21] proposed that  $P$  and  $U$  are related to the effective weight of the caisson. That is  $P = C_h W'$  and  $U = C_u W'$ . Typical values of wave coefficients are  $C_h = 0.4-0.6$  and  $C_u = 0.01-0.4$ , depending on the design wave characteristics and water depth.

The yield wave coefficient is determined when the factor of safety against direct sliding is equal to unity:

$$C_{hy} = \mu(1 - C_u) \quad (32)$$

The permanent sliding of the caisson is obtained by double integrating the equation of motion:

$$x = \frac{W'}{W + W_a} \int \int (C_h - C_{hy}) g \cdot dt \quad (33)$$

where  $W$  is the total weight of the caisson,  $W_a$  is the added

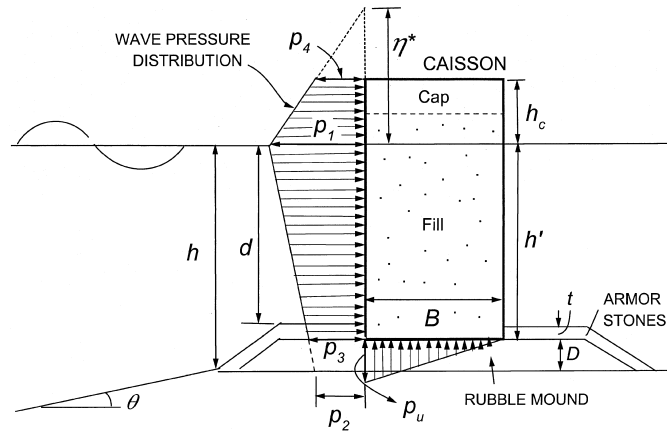


Fig. 9. Sliding of composite breakwater.

mass that may be taken as 20% of the total weight of the caisson.

The procedure to determine permanent displacement of composite breakwater has been verified with 35 case histories [21].

**8. Simplified procedure for vertical acceleration**

The equations to determine permanent displacement require  $k_{hy}$  and therefore  $k_v$ , which varies with time. The procedure implies that a separate set of vertical acceleration record is needed in addition to that of horizontal acceleration (Fig. 2(a)). However, the vertical acceleration may be considered in a simplified manner using a ratio of peak vertical seismic coefficient to peak horizontal seismic coefficient. That is,  $\lambda = k_{vo}/k_{ho}$ . The vertical acceleration is thus assumed to be in phase with the horizontal acceleration.

For the horizontal block, rock block and reinforced soil block, the yield seismic coefficients and displacement correction factors are rewritten as below for the simplified analysis.

- Block sliding along horizontal plane:

$$k_{hy} = \frac{\tan\phi}{1 + \lambda \tan\phi} \tag{1'}$$

$$x = (1 + \lambda \tan\phi) \int \int (k_h - k_{hy})g \cdot dt \tag{2'}$$

- Block sliding along inclined plane:

$$k_{hy} = \frac{\tan(\phi - \Psi_p) + \frac{C}{\eta W}}{1 - \lambda \tan(\phi - \Psi_p)} \tag{7'}$$

$$l = [1 - \lambda \tan(\phi - \Psi_p)] \eta \int \int (k_h - k_{hy})g \cdot dt \tag{11'}$$

- Reinforced soil:

$$k_{hy} = \frac{W_B C_{ds} \tan\phi + W_A \tan(\phi - \alpha) \Lambda}{W_B (1 + \lambda C_{ds} \tan\phi) + W_A [1 + \lambda \tan(\phi - \alpha)] \Lambda} \tag{18'}$$

$$x = (1 + \lambda C_{ds} \tan\phi) \int \int (k_h - k_{hy})g \cdot dt \tag{2''}$$

Note that Eqs. (2') and (2'') are the same since  $C_{ds} \tan\phi$  represents the angle of friction of the soil-geosynthetic interface. The simplified approach to include vertical acceleration has been demonstrated against limited cases of application [20].

**9. Conclusions**

This paper discussed application of sliding block theory to different geotechnical structures. Relevant equations for the yield seismic coefficients and permanent displacement were presented. The equations presented for seismic stability degenerate to that of static stability in the absence of earthquake. A simplified procedure to include vertical acceleration was presented for yield acceleration and permanent displacement. The permanent displacement would be a more rational criterion for performance-based geotechnical design under high seismic load, as witnessed by the recent practice in Japan.

**Acknowledgements**

Materials presented in this paper were completed while the author was supported in part by the National Science Foundation under Grants No. CMS-0084449, CMS-9523141, and INT-9996230 with Richard J. Frigaszy, Priscilla P. Nelson and Larry H. Weber as respective program directors.

## References

- [1] Chang C-J, Chen W-F, Yao JTP. Seismic displacements in slopes by limit analysis. *Journal of Geotechnical Engineering, ASCE* 1984;110(7):860–74.
- [2] Franklin AG, Chang FK. Permanent displacement of earth embankments by Newmark sliding block analysis. Miscellaneous Paper S-71-17, Soil and Pavement Laboratory, US Army Engineer Waterways Experiment Station, Vicksburg, MS, 1977.
- [3] Giroud JP, Beech JF. Stability of soil layers on geosynthetic lining systems. *Proceedings of Geosynthetics Conference, International Fabrics Association*, 1989. p. 35–46.
- [4] Goda Y. New wave pressure formulae for composite breakwaters. *Proceedings of 14th International Conference on Coastal Engineering, ASCE*, 1974. p. 1702–20.
- [5] Goodman RE, Seed HB. Earthquake-induced displacements in sand embankments. *Journal of Soil Mechanics and Foundations Division, ASCE* 1966;92(2):125–46.
- [6] Haynes ME, Franklin AG. Rationalizing the seismic coefficient method. Waterways Experiment Station, Corps of Engineers, Vicksburg, MS 39180, Miscellaneous Paper GL-84-13, 1984.
- [7] Hoek E, Bray J. *Rock slope engineering*. London: Institute of Mining and Metallurgy, 1977.
- [8] JGS. *Proceedings of 34th Japan National Convention on Geotechnical Engineering*, Tokyo, vols. 1–2, Japanese Society of Geotechnical Engineering, 1999.
- [9] JSCE. Proposal on earthquake resistance for civil engineering structures (Special Task Committee of Earthquake Resistance of Civil Engineering Structures), The 1995 Hyogoken-Nambu earthquake investigation into damage of civil engineering. *Earthquake Engineering Committee, Japan Society of Civil Engineers*, 1996, p. 297–306.
- [10] Koerner RM, Hwu BL. Stability and tension considerations regarding cover soils on geomembrane lined slopes. *Geotextiles and Geomembranes* 1991;10(4):335–55.
- [11] Koseki J, Tatsuoka F, Munaf Y, Tateyama M, Kojima K. A modified procedure to evaluate active earth pressure at high seismic loads. *Special Issue of Soils and Foundations* 1998;209–16.
- [12] Leshchinsky D, Boedeker RH. Geosynthetic reinforced earth structures. *Journal of Geotechnical Engineering, ASCE* 1989;115(10):1459–78.
- [13] Leshchinsky D, San K-C. Pseudostatic seismic stability of slopes: design charts. *Journal of Geotechnical Engineering, ASCE* 1994;120(9):1514–32.
- [14] Leshchinsky D, Ling HI, Hanks G. Unified design approach to geosynthetic reinforced slopes and segmental walls. *Geosynthetics International* 1995;2(5):845–81.
- [15] Ling HI, Leshchinsky D. Seismic performance of simple slopes. *Soils and Foundations* 1995;35(2):85–94.
- [16] Ling HI, Leshchinsky D. Seismic stability and permanent displacement of landfill cover systems. *Journal of Geotechnical and Geoenvironmental Engineering, ASCE* 1997;123(2):113–22.
- [17] Ling HI, Cheng AH-D. Rock sliding induced by seismic force. *International Journal of Rock Mechanics and Mining Science* 1997;34(6):1021–9.
- [18] Ling HI, Leshchinsky D, Mohri Y. Soil slopes under combined horizontal and vertical seismic accelerations. *Earthquake Engineering and Structural Dynamics* 1997;26:1231–41.
- [19] Ling HI, Leshchinsky D, Perry EB. Seismic design and performance of geosynthetic-reinforced soil structures. *Geotechnique* 1997;47(5):933–52.
- [20] Ling HI, Leshchinsky D. Effects of vertical acceleration on seismic design of geosynthetic-reinforced soil structures. *Geotechnique* 1998;48(3):347–73.
- [21] Ling HI, Cheng AH-D, Mohri Y, Kawabata T. Permanent displacement of composite breakwater subject to wave impact. *Journal of Waterways, Port, Coastal and Ocean Engineering, ASCE* 1999;125(1):1–8.
- [22] Ling HI, Mohri Y, Kawabata T. Seismic stability of sliding wedge: extended Francais–Culmann’s analysis. *Soil Dynamics and Earthquake Engineering* 1999;18(5):387–93.
- [23] Makdisi FI, Seed HB. Simplified procedure for estimating dam and embankment earthquake-induced deformations. *Journal of Geotechnical Engineering, ASCE* 1978;104(7):849–67.
- [24] Marcuson WF. An example of professional modesty. *The earth, engineers and education, MIT*, 1995. p. 200–2.
- [25] Newmark NM. Effects of earthquakes on dams and embankments. *Geotechnique* 1965;15(2):139–59.
- [26] Richards R, Elms DG. Seismic passive resistance of tied-back walls. *Journal of Geotechnical Engineering, ASCE* 1992;118(7):996–1011.
- [27] Sarma SK. Seismic displacement analysis of earth dams. *Journal of Geotechnical Engineering, ASCE* 1981;107(12):1735–9.
- [28] Seed HB, Goodman RE. Earthquake stability of slopes of cohesionless soils. *Journal of Soil Mechanics and Foundations Division, ASCE* 1964;90(6):43–73.
- [29] Whitman RV. Seismic design and behavior of gravity retaining walls. *Proceedings of Conference on Design and Performance of Earth Retaining Structures, ASCE*, 1990. p. 817–42.